Measurement and models of electron-energy-loss spectroscopy core-level shifts in nickel aluminum intermetallics

David A. Muller
School of Applied and Engineering Physics, Cornell University, Ithaca, New York 14853
and Bell Laboratories, Lucent Technologies, Murray Hill, New Jersey 07974

Philip E. Batson
IBM Thomas J. Watson Research Center, Yorktown Heights, New York 10598

John Silcox
School of Applied and Engineering Physics, Cornell University, Ithaca, New York 14853
(Received 3 February 1998)

Absolute measurements of the *L*-edge core-level binding energies are made for nickel-aluminum compounds using electron-energy-loss spectroscopy (EELS). The core-level shifts are found to compare favorably with *ab initio* calculations of the valence band shifts. The measured EELS oscillator strengths and core-level shifts are used to test the local charge neutrality (LCN) approximation to self-consistency in extended Hückel tight-binding calculations. Within the LCN approximation, the tight-binding calculations can provide estimates of both the core-level shifts and, with the use of the force theorem, the alloy heats of formation for the Ni-Al intermetallics. [S0163-1829(98)04341-0]

I. INTRODUCTION

The threshold of an EELS (electron-energy-loss spectroscopy) edge occurs at the energy required to create a core hole and to add an electron to the lowest-lying excited state of the system. This is the same energy (and electronic configuration) as the XPS (x-ray photoelectron spectroscopy) binding energy in a metallic system with a well defined Fermi energy. However, fewer studies of core-'level shifts have been performed with EELS than with XPS as the fine structure of an EELS edge above the threshold energy can complicate the determination of the precise binding energy. We overcome this difficulty in the EELS measurements by comparison with both first-principles calculations and existing XPS data. Our interest in EELS core-level shifts is motivated by recent atomic-scale EELS measurements of electronic structure changes at grain boundaries in Ni_3Al which were strongly correlated with changes in the mechanical properties of those interfaces.[1] Extensive studies of the trends in XPS core-level binding energies have been undertaken for the intermetallic alloys.[2,3] Rarely do the core levels shift more than an eV (out of a few hundred eV's binding energy) in these metallic systems. This is in marked contrast to the core-level shifts between insulating compounds which can typically be 5–10 eV.[4]

The core-level shift in insulators can often be correlated with the formal valence of the ion.[5] This has encouraged the popular interpretation of core-level shifts as measures of charge transfer.[6] In this traditional explanation, charge transfer from an atomic site leads to a more attractive potential for the core electron, increasing its binding energy, while a charge transfer onto an atomic site reduces the core-level binding energy. This is a gross oversimplification (see Watson *et al.*[7] or Anderson *et al.*[8]), ignoring both the ambiguity in defining the charge transfer and the final state screening of the core hole. For instance, of the eight binary alloys systems studied by Steiner and Hüfner,[9] half had core-level shifts of the same sign for both atomic constituents. The simple interpretation would require that both atomic species had lost or gained charge. Consequently, a core-level shift does not necessarily imply that a charge transfer (assuming that the charge transfer can even be defined) has occurred. Further, the signs of core-level shifts are opposite to those expected from electronegativity arguments.[3,10]

Even in ionic solids, the situation is more complicated than the charge transfer interpretation suggests. A detailed theoretical analysis of XPS core-level shifts in copper-oxides[11] has shown that although the Cu core-level shift can be correlated with the formal valence of the Cu ion, the variation in the number of $3d$ electrons is small and the net charge is not related to the formal valence (for instance Cu^{3+} had a smaller positive charge than Cu^{1+}). Instead Karlsson *et al.* found the core-level shift correlated more with the shift of the Cu $3d$ band, which was in a direction to reduce the Cu→O charge transfer and maintain an approximate charge neutrality. The same concept is also relevant for metallic systems.[12–14]

Core-level shifts can occur even when the charge on each valence orbital is fixed. For instance, if the valence band width is increased, the position of the center of the valence band with respect to the Fermi energy will change (as the number of electrons remains unchanged). A shift in the position of the valence band implies a change in the local potential, which is also experienced (to some extent) by the core electrons. Consequently if the valence band shifts down, we might expect the core states to do so as well. If the valence band is more than half filled, then increasing the band width will increase the core-level binding energy (and the center of the valence band must drop further below the Fermi level) while if the valence band is less than half filled,

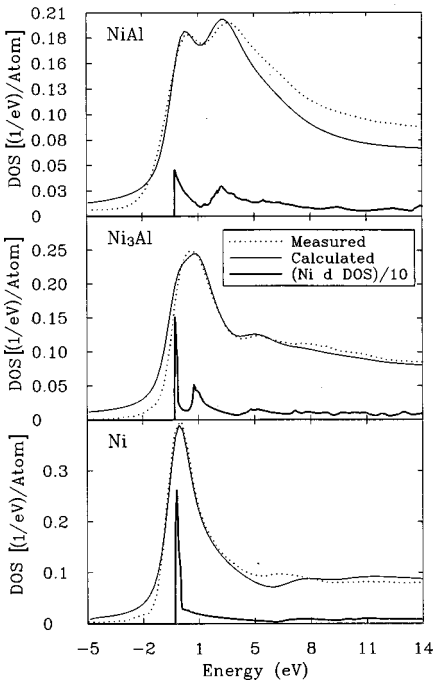

FIG. 1. Comparison of the theoretical (LAPW) and measured Ni L_3 EELS edges for the $Ni_{(1-x)}Al_x$ system (Ref. 18). The oscillator strength (dark solid line) is proportional to the Ni *d* density of states. Lifetime and instrumental broadening of the calculation (light solid line) is described in Muller *et al.* (Ref. 18). The good match between theory and experiment, especially at the edge onset, suggests that distortion due to the core hole is small and the shape of the Ni *L*-edge is determined predominantly by the ground state density of states.

increasing the band width will reduce the core-level binding energy.[12–14] Citrin *et al.*[12,13] and Eastman *et al.*[14] have used this argument to explain the change of sign in surface XPS core-level shifts across the transition metal series. That the core-levels do follow the shifts in the valence band has also been noted by other groups[7,8,15] although they find that errors in ignoring the ''final state effects'' are on the order of 0.1 eV. For the present EELS measurements, this is comparable with the experimental precision, and so is not yet of great concern, but it may become so as experimental accuracy improves.

Three approximations have been made in the above discussion. First, the use of the core and valence states are inherently single-particle descriptions. In Sec. II we use the force theorem of Pettifor,[16] Mackintosh and Anderson[17] to relate core-level shifts (which are determined by differences in the total energy of the system) to shifts in the single-particle eigenvalues for the core states. Secondly, the exchange with, and relaxation around the core have been ignored in the discussion (they are included in Sec. II). Instead, in the discussion, the core-level shift was assumed to result predominantly from the changes in the ground state valence electron distribution. For the present work, we can motivate this approximation by the close correspondence of the measured Ni *L*-edge oscillator strength to the calculated ground state local density of states[18] (DOS) (Fig. 1). This is a stricter condition than is necessary to predict the core-level shift, for which it is only required that the core hole relaxation energies are comparable. The error in ignoring the core hole relaxation is probably about 0.1 to 0.2 eV in comparing a measurement from a surface atom with one in the bulk (Weinert and Watson[7] gives the case for Cu and Anderson *et al.*[8] consider Pd, both of which are less effectively screened than Ni, having lower DOS at the Fermi energy). The change in screening from bulk to surface (in part due to the induced surface dipole layer) is probably more extreme than from bulk to a dislocation or grain boundary, both of which are surrounded by bulk material. The contribution from core hole relaxation is then likely to be smaller than the other systematic errors in the models or the experimental measurements.

The third approximation is the already mentioned correlation between the core and valence band shifts. We investigate this for the bulk Ni-Al compounds by comparing the measured Ni *L*-edge (EELS) core-level shifts to shifts in the center of the *d* band that have been determined self-consistently with *ab initio* LMTO (linear muffin-tin orbital) calculations.

The agreement between the core and valence band shifts is sufficiently good that we can test the validity of the local charge neutrality (LCN) approximation[19–21] for tight-binding calculations of Ni-Al alloys. In a previous paper,[18] we noted that although the shape of the EELS Ni *L* edge changed dramatically across the Ni-Al compounds, the integrated *L*-edge cross section did not. As the EELS oscillator strength is proportional to a local density of states projected onto an atomiclike basis set, this implies that the occupancy of Ni *d* states (for a linear combination of atomiclike orbitals), did not change by more than 2% for a wide range of Ni-Al concentrations. This suggested that a simple approximation to ensure self-consistency in a tight binding calculation is to keep the charge on each orbital fixed upon alloying. This is one form of a local charge neutrality approximation. (Another is to keep the charge on each atom constant.)

An immediate consequence of the LCN approximation is that the self-consistent shift of the valence-band on-site energies to ensure LCN will cause the associated core-level to shift as well. The sign and magnitude of the core-level shifts are physically measurable quantities and we test the predictions of the LCN approximation against the experimental measurements. The tight-binding method used is the extended Hückel (EHT) method,[22] which has as its chief advantage a very small set of free parameters, which need be fitted only to the pure elements. No additional cross terms need to be fitted to model an alloy. An additional test of the method is the use of the force theorem to calculate the alloy heats of formation from the EHT calculations.

This paper is organized as follows. In Sec. II we introduce the framework we use for calculating core-level shifts. In Sec. III we describe the *ab initio* calculations used to calculate the self-consistent shifts of the valence bands upon alloying. The EHT calculations, and their predicted alloy heats-of-formation and core-level shifts are also given. The experimental method and analysis of the systematic errors in measuring core-level shifts from EELS are presented in Sec. IV. The comparison of the theoretical and experimental core-level shifts, and a discussion of the consequences for the LCN approximation are given in Sec. V. The EHT parameters and the tight-binding DOS can be found in the Appendix.

II. CORE-LEVEL SHIFTS AND THE FORCE THEOREM

In a single particle picture for a metal, the EELS threshold is simply the binding energy of the core-level with respect to the chemical potential (or the Fermi level at 0 K). The many-body case is more complicated. Koopmans' theorem identifies the Hartree-Fock (HF) eigenvalues with the ionization potentials of the system for which the Hartree-Fock equations were solved.[23] Consequently the same identification of the ionization potentials cannot be made for the Kohn-Sham eigenvalues of a density-functional theory[24] such as the local density approximation (LDA). The difference between the HF and LDA eigenvalues is (to first order in respective self-energies), the difference between the HF exchange potential and the LDA exchange-correlation potential. This is of the same order as the correlation energy (defined as the energy difference between the HF and the *exact* total energies). The Ni L shell contribution to the correlation energy is on the order of ten eV. This will be the order of the error in using the $2p$ eigenvalues obtained from LDA as the L edge ionization energies (and typically the LDA value will be an underestimate). Unfortunately the core-level shifts are very much smaller than this.

Instead, the smallness of the shifts makes possible their calculation using the force theorem.[16,17] The force theorem provides a simple but still many-body expression for calculating small changes in total energy, even when the total energies themselves are large. This becomes relevant when we note that the core-level binding energy E_B is defined as

$$E_B = E^*_{\rm tot} - E_{\rm tot}, \tag{1}$$

where $E_{\rm tot}$ is the total energy of the ground state and $E^*_{\rm tot}$ is the total energy of the final state. Now the force theorem states that given a self-consistent solution to the Kohn-Sham equations (which can be readily obtained for the ground state), the first order change in total energy, δE, is given by

$$\delta E = \delta\left(\sum_i n_i \epsilon_i \right) + \delta E_{\rm es}. \tag{2}$$

The first term is the change in the occupied one-electron states of energy ϵ_i and occupancy n_i, calculated using the displaced (by the perturbation) but otherwise frozen one-electron potentials. $\delta E_{\rm es}$ is the change in the classical electrostatic energy. If the cell defining the perturbed atom were neutral and spherically symmetric then $\delta E_{\rm es}$ would be zero. Otherwise it would be the change in the Madelung energy. For the former case, the first order *change* in the total energy is given simply by the change in the Kohn-Sham single particle eigenvalues. (Even though the total energies are not given by the eigenvalue sums). The main consequence of the force theorem is that the so called ''double counting'' terms in the Coulomb energies have been canceled out. Although these exchange and correlation energies do make an important contribution to the total energy of the solid, they do not contribute to a first order change in the total energy. The change in total energy of interest here is the transition to the excited state. Further discussion of the force theorem can be found in Heine[25] or Sutton and Baluffi.[26]

Provided the excited states are confined within the same cell as the initial states, the electrostatic contributions, $\delta E_{\rm es}$, will cancel. *Ab initio* calculations of core hole effects in Fe[27] and Co, Ni[28] show the changes between the initial and final states are largely confined to the excited atom. This should be the case in most metals, where the screening length is smaller than the Wigner-Seitz radius[29].

The creation of a core hole is then essentially a promotion energy, which in the framework of the force theorem can then be written as

$$E_B \approx \sum_i \delta n_i \epsilon_i + \frac{1}{2} \sum_i \delta n_i \delta \epsilon_i, \tag{3}$$

where the second order term is also retained, as the relaxation energy $\delta\epsilon_i = \epsilon_i^* - \epsilon_i$ is not small. (For a free Ni atom, the exact (within LDA) binding energy [Eq. (1)] for the transition $2p^6 3d^8 4s^2 \rightarrow 2p^5 3d^9 4s^2$ is 855.172 eV. The first order estimate of the binding energy $\Sigma_i \delta n_i \epsilon_i$ is 834.99 eV. The second order correction of $\frac{1}{2}\Sigma_i \delta n_i \delta\epsilon_i$ is 20.49 eV, which brings the perturbative estimate to within 0.3 eV of the total energy calculation.)

The excitation creates a single core hole, for instance on state j, so $n_j^* = n_j - 1$ and $\delta n_j = -1$. The core electron is excited to the Fermi level (in a metal), increasing the occupancy of a state there, which we label f, so $\delta n_f = +1$. The occupancy of all the other eigenstates of the frozen potential are unchanged so their $\delta n = 0$. We choose to measure all energies with respect to the Fermi level, i.e. $\epsilon_f = 0$ (as the choice of reference energy is arbitrary). With this choice, and the simplified notation, Eq. (3) can be rewritten as

$$E_B \approx -\epsilon_j + \frac{1}{2} \sum_i \delta n_i \delta \epsilon_i. \tag{4}$$

A similar result has been obtained for the Hartree-Fock Hamiltonian by Hedin and Johansson[30] although it should be noted that the Kohn-Sham eigenvalues used here have different values and interpretations from the Hartree-Fock eigenvalues.

The core-level shift between two different environments (labeled primed and unprimed) is

$$\Delta E_B = E'_B - E_B. \tag{5}$$

The force theorem approximates the difference in core-level binding energies as

$$\Delta E_B \approx (\epsilon_j - \epsilon'_j) + \frac{1}{2}\left(\sum_i \delta n_i \delta \epsilon_i - \sum_i \delta n'_i \delta \epsilon'_i \right). \tag{6}$$

As the relaxation energies are determined largely by the on-site screening (so $\Sigma_i \delta n_i \delta\epsilon_i \approx \Sigma_i \delta n'_i \delta\epsilon'_i$), the second term is expected to cancel itself out. In comparing the core-level shifts for a free Ni atom in the initial states $2p^6 3d^8 4s^2$ and $2p^6 3d^9 4s^1$, we find $(\epsilon_j - \epsilon'_j) = -1.252$ eV, while the relaxation term only contributes -0.028 eV. The core-level calculated using the total energy differences (the ''exact'' answer) is -1.34 eV. The error between the force theorem [both terms of Eq. (6)] and the total energy calculations is then 0.06 eV. If only the first order term is retained in the force theorem estimate, then the error is 0.09 eV. As this is comparable to the expected experimental errors, we will re-

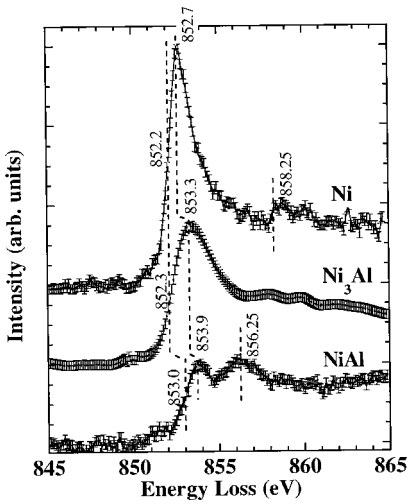

FIG. 2. Measured Ni $L_{2,3}$ binding energies in Ni-Al alloys. Spectra were recorded on the IBM STEM with a Wien filter spectrometer.

tain only the first term, which is simply the difference in the LDA single particle eigenvalues.

While the absolute binding energies cannot be accurately calculated from the ground state LDA single particle eigenvalues alone, the force theorem gives a simple prescription for calculating the *shifts* in binding energy from them (see Fig. 2). Notice that the core-level shift contains both initial state effects [chemical shifts from changes in the ground state such as $(\epsilon_j - \epsilon_j')$] and final state effects [relaxation $(\epsilon_i^* - \epsilon_i)$] due to the presence of the resulting core hole. Although the final state effects are often larger than the chemical shifts,[7] the core-level shift is dominated by the initial state effects. This is because the screening of the core hole is mostly intra-atomic, making the relaxation energy relatively insensitive to changes in the local environment.[11]

III. CALCULATIONS OF VALENCE BAND SHIFTS

The approximation that the core-level shifts will follow shifts in the valence band relies on the core electrons experiencing a similar change in potential to the change experienced by the valence electrons. This is more likely to be satisfied for wave functions such as $3d$ states, which penetrate the atom core, than for valence states which are orthogonal to the inner shell electrons such as the $4s$ or $4d$ states. An immediate implication is that we would expect the approximation to be best obeyed for precisely those materials that do not have soft pseudopotentials (for which orthogonality to the core states is generally required). Consequently we would expect better agreement between core and valence band shifts for the $3d$ transition metals than for the $4d$ or $5d$ series. As the L-edge binding energies are also a lot smaller for the $3d$ series than the $4d$ series, we might also expect that the absolute errors made will be smaller also. In particular, the errors introduced by ignoring final states effects should be smaller.

A. *Ab initio* calculations

The self-consistent linear-muffin-tin-orbital (LMTO) method[31] was used with the local density approximation (LDA) for the exchange and correlation potentials.[24,32] The ratio of sphere radii in the alloys were chosen according to Anderson's prescription,[33] but the choice of different ratios, such as those used by Moruzzi and Marcus *et al.*[34] or Nautiyal and Auluck,[35] resulted in changes of less than 0.05 eV to the valence band shifts and heats of formation. The calculations were much more sensitive to the choice of lattice constant, as the bandwidth can vary rapidly as the fifth power of interatomic spacings.[31] The minimum in LMTO total energy was generally found to occur at lattice constants that were roughly 3% smaller than is measured experimentally. The experimental total energies and valence band widths were typically 0.2 eV less at the experimental lattice constant than at the LMTO energy minimum. However, the *differences* in total energy and valence band shifts were less than 0.03 eV, provided the lattice constant was chosen according to the same prescription (i.e., experimental or LMTO energy-minimum) for all the systems being compared. The results reported here are for the experimentally observed lattice constants.

Ni and Al have fcc structures with lattice constants (for the cubic unit cells) of $6.650a_0$ and $7.651a_0$, respectively. Ni_3Al has the $L1_2$ or Cu_3Au crystal structure of the Al atoms at the corners of a cube and the Ni atoms at the face centers of the cube.[36] The lattice constant is $6.743a_0$. NiAl has the $B2$ or CsCl structure with the Al at the corners of a cube and the Ni atom at the body center.[36] The lattice constant is $5.450a_0$.

Spin polarization was included only for the Ni calculation. Although Ni_3Al is thought to be a weak itinerant ferromagnet,[37] its Curie temperature of 43 K is well below the measurement temperature ($\approx$300 K). For comparison with experiment, Ni_3Al is assumed to be paramagnetic. Simulations of the magnetic properties of Ni_3Al can be found in Refs. 38, 34, 39 and 35. The magnetic effects, even at 0 K, are very weak, and the error made in neglecting them ($\approx$0.003 eV) is much smaller than the energy scale of interest in this work.

The potentials were obtained self-consistently using $286k$ points in the irreducible part of the Brillouin zone for Ni, NiAl, and Ni_3Al. This was roughly double the number of k points required to converge the total energy to 10^{-8} Ry. However, as the calculations can be (and were) performed in a few minutes on a laptop computer, the larger k point sets was used. $1240k$ points in the irreducible part of the Brillouin zone were for the Al calculations, to ensure an adequate sampling close to the zone boundaries and edges. The basis sets included s, p, d, and f orbitals for each site. The densities of states were calculated using the analytic tetrahedron method.[40]

In the atomic sphere approximation (ASA), the center of each l projected DOS, C_l, are defined[41,31] to be the energy at which the logarithmic derivative of the wave function at the sphere boundary is $-l-1$. As the Ni DOS is dominated by the d electron contribution, a weighted average of all the valence C_l's is little different from C_d. Consequently, we use C_d (referenced to the Fermi energy) to measure shifts in the valence band.

We defer a full discussion of the results to Sec. V. However, it should be noted that the shifts in C_d track the measured EELS core-level shifts to within the experimental er-

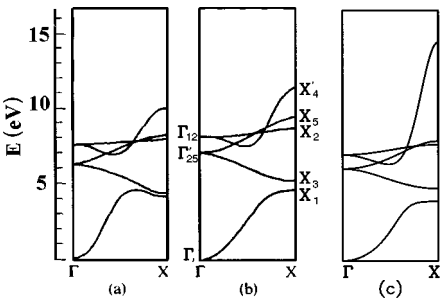

FIG. 3. Comparison of band structures for paramagnetic Ni calculated by (a) orthogonal tight-binding [p. 486 of Harrison (Ref. 67)]; (b) APW (Ref. 71); (c) extended Huckel tight-binding (from this work).

rors. Although more accurate methods of calculating core-level shifts do exist, the interest here is rather to test the simpler theories that connect the core-level shifts to changes in the ground state electronic structure.

B. Extended Hückel tight binding calculations using the local charge neutrality approximation

Having demonstrated that the core-level shifts track the valence band shifts for the Ni-Al compounds, we now ask the next question: *why do the valence bands shift upon alloying?*

We address this by constructing a simpler model of the solid using an extended Hückel tight-binding theory, which is described more fully in Appendix A (see Fig. 3). The extended Hückel theory (EHT) is one of the more popular semiempirical tight binding methods used in quantum chemistry. Originally used by Wolfsberg and Helmholtz in modeling inorganic complexes,[42] the method was further developed and widely applied by Hoffman.[22] A survey of most of the chemistry using EHT can be found in Ref. 43.

The force theorem [Eq. (2)] suggests that a tight binding model should be able to provide a description of the cohesive energy of a solid, provided the reference system is chosen with care. The tight binding bond model[44,45,20,46] (TBB) gives a clear prescription of how to do so, and attaches physical interpretation to what are otherwise apparently *ad hoc* corrections to the tight-binding formalism. Applying the force theorem, as in Sec. II, the cohesive energy of a solid can be written as

$$U_{\mathrm{coh}} = U_{\mathrm{bond}} + U_{\mathrm{prom}} + \delta E_{\mathrm{es}}. \tag{7}$$

If the reference system chosen is a free atom with orbitals at energies $\{\epsilon_i\}$ then the bond energy can be rewritten as[20]

$$U_{\mathrm{bond}} = \sum_i \int_{-\infty}^{E_F} (E-\epsilon_i) n_i(E)\, dE, \tag{8}$$

where $n_i(E)$ is the i projected LDOS and E_F is the Fermi energy (for simplicity only metals at $T=0$ K are considered—a Fermi function must be introduced at finite temperatures). This describes the covalent bonding that occurs when the solid is formed from the free atoms.

The promotion energy U_{prom} takes into account the change in occupancy of the orbitals on forming the solid from the reference system

$$U_{\mathrm{prom}} = \sum_i \delta n_i \epsilon_i. \tag{9}$$

Together, $U_{\mathrm{bond}} + U_{\mathrm{prom}}$ can be identified as the first term of the force theorem [Eq. (2)]. If the system is kept charge neutral then these will be the only contributions to the force-theorem calculated binding energy.

EHT is most successful for compounds formed from elements of similar electronegativity.[47] This is because the lack of self-consistency and electron-electron interactions in the standard EHT leads to a large overestimation of the charge transfers between elements with dissimilar electronegativies. An electron-electron term of the form $U_{\mu\nu}Q_\mu Q_\nu$ can be added to the Hamiltonian which leads to a tight-binding Hartree model.[48] $U_{\mu\nu}$ is the effective intrasite Coulomb interaction and Q_μ is the charge associated with the μth orbital. An alternative approach, more common in the chemistry community, is to add the Coulomb integral to the diagonal matrix elements of the Hamiltonian.[49] In both cases, a self-consistent solution is found through iteration, the effect of which is to greatly reduce the charge transfers. For instance, in tight-binding Hartree calculations of the Ni-Al phase diagram,[50,51] the charge transfer did not exceed $0.1e^-$. For d electrons, the Coulomb integrals are of the order of 10 eV, which is much larger than any of the heats of formation for the metal alloys. It is not then a very drastic approximation to set the Coulomb integrals to infinity. This has the effect of making the charge on each site in the alloy to be the same as in the reference system (and has the advantage of reducing the number of fitting parameters in the Hamiltonian). The simplest modeling of this self-consistency is to impose a local charge neutrality on the system. This can be done by either rigidly shifting all the diagonal Hamiltonian matrix elements on a given atom by the same amount[19,20] or by adjusting the individual atomic orbital[21] (in which case the promotion energy is zero). In both cases, the calculation must be iterated to self-consistency. From the force theorem we know that a self-consistent redistribution of charge does not contribute to the force on the atom so the bond energy is calculated with respect to the self-consistently determined on-site energies.

In the present work, the EHT is used as a framework to implement the tight-binding bond model so no special significance is attached to the Slater-type orbitals. They are regarded as parameters to be fitted to bulk band structures. The modifications necessary to convert EHT to a TBB model are as follows.

The matrix elements of the Hamiltonian are fitted to reference band structures (e.g., from LMTO calculations) for the pure elements. This allows the force theorem to be used to estimate the energy changes upon alloying.

Local charge neutrality is imposed on each orbital, i.e., an orbital in the alloy must have the same number of electrons as it did in the reference system. The diagonal matrix elements are iteratively adjusted until charge neutrality is reached. ($H'_{ii} = H_{ii} + \lambda\, \delta Q_i$ where the mixing constant λ is of order unity.) Typically 10–15 iterations are needed to converge the charge imbalance, δQ_i, to less than $0.01e$.

The bond energies $\Sigma_i n_i (E_i - H_{ii})$, not the band energies $\Sigma_i n_i E_i$, are used to calculate changes in the total energy. In accordance with the TBB model, the self-consistent readjust-

ment of H_{ii} does not change the total energy. There are also no contributions from the promotion or electrostatic energies as the system remains strictly charge neutral.

It was found that keeping each orbital charge neutral, rather than just each atom, improved the calculated heats of formation by a factor of 4. This may be an artifact of the EHT method as the hopping parameters (off-diagonal H_{ij}) are affected by changes of H_{ii} on an absolute energy scale. It may also reflect the difference in Coulomb integrals for the Ni *s* and *d* states. If the *s*-*d* energy difference was kept fixed on alloying there would be a significant redistribution of charge between the Ni *s* and *d* states, even if the total charge per Ni atom was kept fixed. As $\epsilon_d \approx \epsilon_s$ in the EHT fit, the promotion energy is small, and comparable to the Coulomb integrals neglected by the force theorem. Consequently, the energy cost of the *s*-*d* transfer cannot be accurately determined, a problem which the orbital neutrality condition avoids.

The crystal structures and lattice constants are the same as those used in the LMTO calculations of the Ni-Al system. A cubic supercell was used for all calculations so the same set of 200*k* points in the irreducible Brillouin zone could be used when calculating the DOS. The Hoffman group EHT package *YAeHMOP*, written by Greg Landrum (1994), was used.[52] The EHT parameters and DOS are given in the Appendix.

C. Results

EHT parameters were fitted only for bulk Ni and Al (Appendix A). No changes or new parameters are introduce in the calculation of the alloys, other than the requirement of local charge neutrality and the use of the experimental lattice constants. The calculated alloy DOS, heats of formation ΔH, and shifts in band energies are then predictions of, rather than fits to, the properties of the alloys themselves. The ultimate test of the method is how well the calculations agree with experiment.

There are two tests of the local charge neutrality (LCN) approximation we can perform on our tight-binding calculations. First, the experimentally measured core-level shift should match the valence band shift required to keep the charge per orbital unchanged during alloying. Secondly, the force theorem can be applied to the calculated DOS to estimate the alloy heats of formations. The extended Hückel method provides a useful framework for both these tests as the semiempirical tight-binding parameters need only be fitted to pure elements and not the alloys of interest.

The DOS for the various Ni-Al alloys are shown in Fig. 4. The Ni *d* band appears to shift lower in energy with increasing Al concentration, yet the number of *d* electrons is fixed. This implies that in some sense, the *d* DOS is being broadened as the system is made increasingly Al rich. At the same time the sharply peaked central portion of the atomic *d* DOS appears to become narrower. The overall effect is to transfer states from the centroid to the tails of the DOS (i.e., increase the 4th moment of the *d* DOS). Both these trends can be understood in terms of the loss of Ni *d*-*d* interactions and increased *s*-*d* hybridization.[53,18]

The STO's for Ni, Al as well as the self-consistent ionization potentials for NiAl and Ni_3Al have already been given in Table VII. The ionization potentials should not be interpreted on an absolute scale—removing an electron to infinity in a real solid would involve a calculation of the dipole potential present at the surface. Instead, the chemical potential of the solid can be used as a meaningful reference energy. (This is the Fermi energy as the calculations are for metals at 0 K.) This is also the quantity that is measured with EELS while the ionization energy has no special significance in EELS and cannot be directly determined.

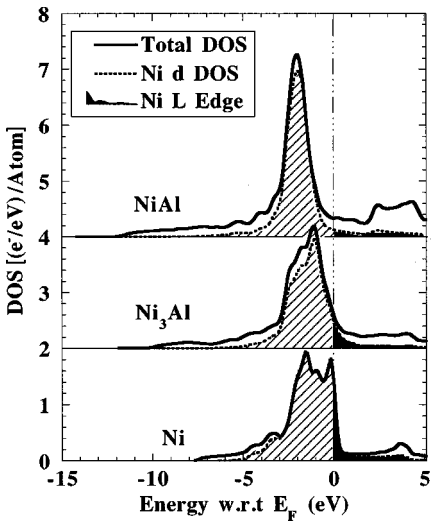

FIG. 4. EHT calculated density of states for the Ni-Al compounds. The atomic *d* DOS is indicated by the shaded area and the unoccupied portion of the *d* DOS (which determines the shape of the Ni EELS *L* edge) is represented by the solid area. Although the *d* band appears to shift to a lower energy as Al is added to Ni, the number of *d* electrons remains the same.

When the band centers (first moment of the LDOS) are measured with respect to the Fermi energy (Table I), the effects of the local charge neutrality can be seen. The Ni *d* band has shifted further below the Fermi surface while the Al band centers have shifted up. A shift of the valence band with respect to the Fermi level also implies that the core levels must be shifted. For orbital charge neutrality, the core shift is the weighted average of the valence levels. The core-level shifts due to orbital charge neutrality are in very good agreement with the experimental core-level shifts reported in Sec. IV.

The tight-binding bond energies obtained from Eq. (8) are given in Table II. This is the only term that will contribute to the force theorem estimate of the heats of formation of the alloys:

TABLE I. EHT band centers measured with respect to the Fermi energy in the Ni-Al compounds (in eV).

	Ni		Al	
	$\mu_s^1 - E_F$	$\mu_d^1 - E_F$	$\mu_s^1 - E_F$	$\mu_p^1 - E_F$
Ni	−0.85	−1.18		
Ni_3Al	−0.40	−1.24	−2.12	+2.15
NiAl	+0.45	−1.59	−2.19	+2.29
Al			−2.75	+1.77

TABLE II. EHT bond energies and alloy heats of formation, ΔH. The LMTO-ASA calculations of ΔH from this work are similar to the ASW calculations of Hackenbrackt *et al.*[38] The experimental ΔH is from Hultgren *et al.*[84] All energies are in eV.

	U_{bond}	EHT ΔH	Experimental ΔH	LMTO-ASA ΔH	ASW ΔH
Ni	−1.964				
Ni_3Al	−2.962	−0.31	−0.38±0.05	−0.48	−0.47
NiAl	−4.051	−0.72	−0.61±0.05	−0.76	−0.74
Al	−4.698				

$$\Delta H(\mathrm{Ni}_{1-x}\mathrm{Al}_x) \approx U_{\text{bond}}(\mathrm{Ni}_{1-x}\mathrm{Al}_x) - xU_{\text{bond}}(\mathrm{Ni}) - (1-x)U_{\text{bond}}(\mathrm{Al}). \quad (10)$$

The EHT calculations overestimate the experimental heat of formation by approximately 0.1 eV for Ni-Al and underestimate it by 0.1 eV for Ni_3Al. The EHT heats of formation would be reduced by approximately 0.05 eV if magnetic effects were included. The errors in the EHT estimates are (probably fortuitously) no worse than those in the *ab initio* calculations of Hackenbracht and Kubler[38] or the LMTO-ASA calculations of Sec. III A, both of which consistently overestimate the heat of formation by about 0.1 eV. If the EHT parameters for the bulk materials were used directly in the alloy calculations, without correcting the charges self-consistently, then the Ni-Al heat of formation is overestimated by 0.4 eV. Self-consistency, even when approximated by local charge neutrality, seems to be an important factor in describing the trends in cohesive properties.

The good agreement between the EHT calculations and the experimental heat of formation raises an interesting point: As no charge transfers were allowed in the EHT model, the stability of the alloys is predominantly the result of covalent bonding. The ionic contribution is not important for considering the phase stability. Instead, it is sufficient to consider only the changes in the LDOS when estimating changes in cohesion. This will prove to be very useful in relating the EELS measurements to grain boundary energies.

D. Summary

The tight-binding bond approach to the EHT model has successfully reproduced the heats of formation and the core-level shifts for the Ni-Al compounds studied, to within 0.1 eV. Only bulk Ni and Al parameters were fitted but the alloy cohesive properties and DOS trends were accurately predicted. This was only possible when local charge neutrality was imposed on the system and energies were measured using the force theorem.

IV. EXPERIMENTAL METHOD

Details of the specimen preparation and processing of the recorded spectra are the same as those described previously.[18] The effects and prevention of electron beam radiation damage in the Ni-Al system can be found in Muller and Silcox.[54]

A. Specimen preparation

Electron spectroscopy in a scanning transmission electron microscope (STEM) is performed in a transmission mode, usually with a small focused probe.[55] An additional advantage of spectroscopy in an electron microscope is that the specimen can be imaged and regions with obvious defects can be examined separately. The high lateral spatial resolution[56–58] (2–8 Å) means the specimen need only be defect free over distances as small as a few nanometers. Of course, very much larger areas are used to avoid finite size effects.

Al thin films were deposited directly onto formvar grids by magnetron sputtering. This meant only one surface of the film was exposed to atmosphere when the specimens were transferred to the STEM. The nominal mass thickness was 20 nm but grains as large as 50 nm were observed. The Al L edges were recorded on these larger grains where the surface oxide accounted for less than 5% of the probed volume.

The Ni, Ni-Al, and Ni_3Al specimens were prepared for transmission electron microscopy by jet polishing with a 10% sulfuric acid solution in methanol.

B. Instrumentation

A VG-HB501 STEM equipped with a Wien filter spectrometer[59] was used to measure the EELS spectra of the Ni-Al compounds on an absolute energy scale. The filter floats at the electron beam acceleration voltage of 120 kV so the spectrometer is insensitive to instabilities and drift of the microscope's high voltage supply. By applying a known voltage to the Wien filter, energy losses can be measured on an absolute scale, with a precision of ± 50 meV at the Ni L edge and somewhat better, ± 20 meV at the Al L edge. (The binding energy of bulk Ni spectra, measured six months apart, were also reproduced to within ± 50 meV.) The energy resolution of the spectrometer is about 0.15 eV so the resolution of the spectra is limited by that of the electron source. For low extraction voltages, the resolution of a field emission gun is 0.25 eV. When larger currents are required (as in this work) and a higher extraction voltage is used, the energy resolution is 0.3–0.4 eV. At large energy losses, the signal is dominated by a large background, possibly due to stray electrons from the deflected zero-loss beam striking the side of the spectrometer. This limits the sensitivity of the detector and makes deconvolution of the spectra difficult as the background shape is unknown. While this limits the quantification of EELS cross sections, it has little effect on the position of the edge onsets, and hence little effect on the measured core-level shifts, which are the quantities of interest in this paper.

C. Measuring the core-level binding energy

Although the energy axis for an EELS measurement can be determined on an absolute scale, a precise determination of the core-level binding energy is not always straightforward. The EELS edge has considerable structure which is convolved with the finite resolution of the microscope as well as the core hole lifetime. Consequently the peak of the EEL spectrum need not (and often does not) mark the onset of the spectrum (see Fig. 1).

TABLE III. Modeled Ni L-edge core-level shifts in Ni-Al alloys. The binding energies are determined from the inflection point in the simulated EELS spectra, calculated from the broadened LAPW LDOS. The actual edge onsets are all at 0 eV. ΔE_B is the systematic error in using the inflection point to measure core-level shifts with respect to bulk Ni.

	Binding energy (eV)	ΔE_B (eV)
Ni	-0.39	
Ni_3Al	-0.39	0
NiAl	-0.27	$+0.12$

The definition of our edge onset is somewhat arbitrary, but if a consistent definition is used, the systematic errors will be similar, and can be expected to cancel when measuring the *differences* between edge onsets. The accurate reproduction of the measured EELS edges with LAPW calculations[18] allows us to test various definitions. If the spectrum were a simple step function, then for a symmetric blurring, the binding energy would be given by the inflexion point (the first maximum of dI/dE). This is a stable and well-specified definition of the core-level binding energy. While exact for a step function, it will underestimate the binding energy for a delta-function feature. An estimate of the systematic errors in using the inflexion point can be obtained from treating the LAPW calculated EELS spectra in the same manner as the experimental data which they matched so well (Fig. 1). The results are shown in Table III. As expected, the binding energy is underestimated (by 0.4 eV). However, all the binding energies are all underestimated by a similar amount so the relative error in the core level shift is closer to 0.1 eV. This is comparable to the uncertainty in the experimental data.

An additional attraction of using the inflection point to determine the core-level shift is its insensitivity to errors in the background subtraction of the measured spectra. The background should be slowly varying at the Ni L edge so the error in background slope over the edge onset is first order in the binding energy. Thus it only adds a constant to the derivative of the spectrum. As the inflection point is obtained by a second differentiation, the background does not contribute. The experimental core-level binding reported in Table IV was determined using the inflection point definition.

TABLE IV. Measured Ni L-edge core-level binding energies in the Ni-Al intermetallics. The roughly 0.4 eV difference between the EELS and XPS measurements can be attributed to the use of the inflection point to define the EELS core level binding energy (see Table III).

	EELS L_3 binding energy (eV)	XPS[b] L_3 binding energy (eV)	XPS[a] L_3 binding energy (eV)
Ni	852.2 ± 0.05	852.65 ± 0.2	852.8 ± 0.1
Ni_3Al	852.3 ± 0.05	852.65 ± 0.2	
NiAl	852.9 ± 0.1	852.8 ± 0.2	853.3 ± 0.1

[a]F.U. Hillebrecht *et al.*, Phys. Rev. B **27**, 2179 (1983).
[b]S.C. Liu *et al.*, Phys. Rev. B **42**, 1582 (1990).

TABLE V. Measured Ni L-edge core-level shifts in the Ni-Al alloys. The core-level shifts are referenced to the bulk Ni measurement. From Table III we would expect the measured Ni-Al EELS core-level shift to be overestimated by about 0.1 eV.

	EELS core-level shift (eV)	XPS[a] core-level shift (eV)	XPS[b] core-level shift (eV)
Ni_3Al	0.1 ± 0.07	0.0 ± 0.3	
NiAl	0.7 ± 0.1	0.2 ± 0.3	0.5 ± 0.1

[a]F.U. Hillebrecht *et al.*, Phys. Rev. B **27**, 2179 (1983).
[b]S.C. Liu *et al.*, Phys. Rev. B **42**, 1582 (1990).

V. RESULTS AND DISCUSSION

Table V shows the Ni L_3-edge core-level shifts with respect to bulk Ni. Similar shifts are seen with XPS and EELS although the errors are somewhat larger in the XPS measurements. The systematic errors expected for the EELS measurements (Table III) suggest that the Ni-Al EELS core-level shift may be overestimated by 0.1 eV. Overall the core-level shifts are seen to be small but they are nonzero and do increase with increasing Al concentration.

Table VI shows the core-level shift is found to be in good agreement with that predicted by EHT calculations when local charge neutrality is imposed. The agreement is good (within the 0.1 eV uncertainty of both theory and experiment). This is not unexpected since the calculated ground state DOS agrees well with the shape of the EELS $L_{2,3}$ edges as shown in Fig. 1; see also Muller *et al.*[18]). The agreement for both the core-level shifts and EELS shapes suggest the interactions between the core hole and the valence electrons are weak in this system.

The physical picture of the core-level shift in the TBB model is then that the local densities of states can change shape and width, but that each atom remains neutral. This means that the atomic levels must shift in a direction to reduce the charge transfer and maintain an approximate charge neutrality. The Al L-edge core-level shift is further evidence of this effect. The Al L-edge core-level shift between Al and Ni-Al is $+0.3$ eV and the EHT shift of the Al valence bands with respect to the Fermi energy is $+0.32$ eV. This picture may be applicable to insulators as

TABLE VI. Comparison of the Ni L-edge EELS core-level shifts and calculated valence band shifts in the Ni-Al alloys. The core-level shifts should follow the valence band shifts if the core states experience the same change in potential. The LMTO shifts are with respect to ferromagnetic Ni. The shifts are increased by 0.04 eV when spin polarization is ignored. A positive value is an increased binding energy (or position below the Fermi energy) with respect to fcc Ni. From Table III we would expect the measured NiAl EELS core-level shift to be overestimated by about 0.1 eV.

	EELS core-level shift (eV)	LMTO C_d shift (eV)	EHT valence band shift (eV)
Ni_3Al	0.1 ± 0.07	0.06	0.10 ± 0.1
NiAl	0.7 ± 0.1	0.53	0.52 ± 0.1

well as metal alloys as a similar behavior has been found in the copper-oxide system.[11]

If a system does remain charge neutral (in a tight binding sense) then the sign of the core-level shift can be predicted from the changes in bandwidth that occur on alloying. Since the number of electrons per atom is fixed, an increase in the width of valence DOS associated with a particular atom implies that the average energy of that atom's valence states must lie further below the Fermi energy. As the core levels (of a given atom) follow the average shift of the valence states (on that atom), the core-level binding energy (for that atom) is also increased.

VI. APPLICATION TO OTHER SYSTEMS

The close correlation between the core-level and valence band shifts has been widely used in the analysis of XPS data.[12–15] Quantitative analysis (both for EELS and XPS) is restricted to metallic systems as the core-level shift can only be related to valence band shift if there is a well-defined Fermi energy. As mentioned in the Introduction, the final state contributions are expected to be less severe at internal interfaces than at free surfaces. Generally, if the EELS spectrum reproduces the unoccupied, single-particle density of states then core-hole and final-state effects are likely to be small. In the self-consistent LMTO calculations, the core-level shift was assumed to track the center of the *d* band. Strictly speaking, the core-level shift should track the average valence band shift, weighted by number of electrons and the proximity of their wave functions to the core states. However, most of the electrons in the Ni valence band have a *d*-like character so it was not necessary to make this distinction in the present work. For metals on the left side of the Periodic Table, the contribution from the other electrons is likely to become significant and the average valence band shift should be used.

A far more restrictive approximation is the local charge neutrality imposed on the tight binding calculations in Sec. III B. If small charge transfers do occur, the method will be in error by the neglected difference in Madelung energies [which was discarded in Eqs. (2) and (7)]. As a rough rule of thumb, the charge neutrality approximation will break down when the Pauling ionicity exceeds 10% (Ref. 60) (the Fe:B, Fe:P, Cu:Bi, Ni:Si, and Ni:Al systems all satisfy this rule very comfortably).

EELS core-level shifts have been measured in the Ni:Si system[61] and provided an additional check on these approximations. Nickel silicides have been heavily studied, motivated by their potential applications as Schottky barriers and Ohmic contacts in the microelectronics industry.[62–64] Consequently, XPS core-level shifts have also been published. The Ni $2p$ core level shifts (corresponding to the Ni *L*-edge binding energy) for Ni_2Si and NiSi with respect to Ni are 0.6 and 1.1 eV, respectively[64] (no error bars were given). From EELS, the core-level shifts for Ni_2Si, NiSi, and $NiSi_2$ are 0.5 ± 0.4,1.5 ± 0.4, and 2.5 ± 0.4 eV.[61] Core-level shifts have also been reported for the Ni $3p$ core states (the Ni *M* edge);[65] however, the presence of a strong Fano resonance on the Ni *M* edge[66] is likely responsible for the anomolous behavior reported for Ni_2Si and NiSi.

We find the core-level shift predicted by self-consistent LMTO calculations for Ni_3Si is 0.37 eV, and 0.3 ± 0.1 eV by applying the LCN approximation to EHT (Wong's EELS measurement is 0.5 ± 0.4 eV). For Ni_2Si, LMTO predicts a 2.1 eV core-level shift with respect to Ni, and LCN-EHT predicts a 2.4 ± 0.2 eV core-level shift (Wong's EELS measurement is 2.5 ± 0.4 eV). Given the large change in chemical environment from Ni to $NiSi_2$, the ability to reproduce the experimental core-level shift is very encouraging. (For the EHT calculations, the Ni parameters were the same used for the Ni-Al system described earlier in the paper. The Si parameters were the defaults provided by *yaeht*.[52])

VII. CONCLUSION

The experimental Ni L_3 core-level binding energy was determined from the first inflection point of the EELS spectrum. By testing this definition on modeled core edges for the bulk Ni-Al alloys, it was found that this resulted in a systematic underestimate of the absolute binding energy by about 0.4 eV. The error results largely from the energy resolution of the microscope and the core hole lifetime, which are independent of the Ni atom's environment, and so is largely canceled in the estimate of the core-level *shifts*, as it is a difference in binding energies. The largest error, of 0.12 eV, was in estimating the shift of the Ni L_3-edge between Ni and Ni-Al. This is comparable to the experimental precision, which is limited by the signal to noise ratio in the EELS spectra. The difference between EELS and XPS core-level binding energies can be largely attributed to the different methods required to precisely define the edge onset.

The force theorem provides a framework for calculating the core-level shifts resulting from small perturbations to an atom. In the extended Hückel tight-binding approximation model, the core-level shift is assume to follow the shift of the valence band center with respect to the Fermi energy. The measured core-level shifts with respect to pure Ni for the bulk Ni-Al alloys were found to be within 0.1 eV experimental error of the shifts predicted from the EHT model where local charge neutrality had been assumed. As the shifts are a consequence of the EHT model, and not fitted parameters, this is a successful microscopic test of the thesis that the local charge neutrality is a good approximation (to within 0.1 eV) of the self-consistent screening in bulk Ni-Al alloys.

ACKNOWLEDGMENTS

The research at Cornell was funded by U.S. DOE Grant No. DE-FG02-87ER45322. The use of the materials preparation facilities of the Cornell Materials Science Center which is supported by the NSF is acknowledged (Grant No. DMR-9121654). The Ni_3Al and Ni-Al specimens were provided by Shanthi Subramanian and Alice Wu.

APPENDIX: THE EXTENDED HÜCKEL METHOD AND TIGHT BINDING PARAMETERS

The starting point for the extended Hückel theory (EHT),[42,22] as with most tight binding theories, is the secular equation[67,68]

TABLE VII. Summary of parameters used in the EHT calculations. The STOs are not altered upon alloying but the ionization potentials are adjusted to ensure charge neutrality.

Ionization potentials (eV)				
	Ni		Al	
	ϵ_s	ϵ_d	ϵ_s	ϵ_p
Ni	−9.500	−8.000		
Ni_3Al	−9.721	−7.688	−11.793	−6.424
NiAl	−9.615	−7.781	−12.066	−6.218
Al			−12.3	−6.5

Slater type orbitals						
	ζ_s	ζ_p	$\zeta 1_d$	$c1$	$\zeta 2_d$	$c2$
Ni	2.25		5.75	0.5683	1.90	0.6292
Al	1.55	1.6				

$$\sum_j (H_{ij}-E_m S_{ij})c_{mj}=0, \quad i=1,2,\ldots, \tag{A1}$$

where m labels the eigenstates and i,j label the atomic basis states. The eigenfunctions φ_m are linear combinations of the atomic orbitals, ϕ_i,

$$|\varphi_m\rangle=\sum_i c_{mi}|\phi_i\rangle. \tag{A2}$$

The matrix elements of the Hamiltonian are $H_{ij}=\langle\phi_i|\hat{H}^{\text{eff}}|\phi_j\rangle$ and the overlap integrals are $S_{ij}=\langle\phi_i|\phi_j\rangle$. $\hat{H}^{\text{eff}}$ is the (as yet unspecified) one-electron Hamiltonian. The overlap integrals are central to the EHT method, determining the distance dependence of interactions (both for S_{ij} and H_{ij}). The overlaps are explicitly calculated, using Slater-type orbitals (STO's) for each of the basis states i, rather than fitting the overlap integral to each i,j pair. Consequently, only N sets of parameters are needed for different N types of atoms, rather than the needed N^2 if cross terms were fitted directly. The result is a much smaller set of parameters than a conventional tight-binding fit.

The diagonal matrix elements are taken to be the ionization potentials of a reference system (usually fitted to the single-particle eigenstates of a free atom or a measured ionization energy of a solid)

$$H_{ii}=\epsilon_i. \tag{A3}$$

The parameter set is reduced further by the use of the Wolfsberg-Helmholtz *ansatz* for the off-diagonal matrix elements of the Hamiltonian:[42,69,70]

$$H_{ij}=-K\frac{H_{ii}+H_{jj}}{2}S_{ij}, \tag{A4}$$

where K is a numerical constant, usually between 1 and 3. Hoffman chose $K=1.75$ which was optimized for the comparison of the staggered and eclipsed conformations of ethane.[22] Bisi and Calandra have used $K=2.5$ in their calculations of nickel silicides.[62] In the present work, this modification did not lead to improved fits to band structures so the constant was left at Hoffman's value.

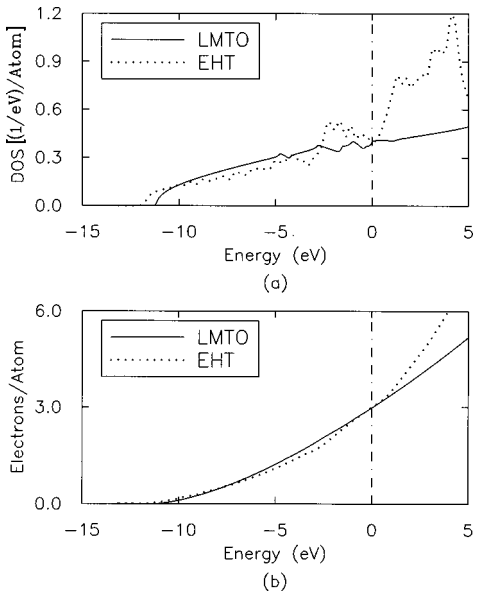

FIG. 5. (a) Comparison of the LMTO DOS for fcc Al (from Sec. III A) with the EHT fitted DOS. (b) The integrated DOS from both calculations. The discrepancies in the integrated DOS are much smaller than the DOS itself.

The EHT parameters were fitted to the band structures of bulk Ni and Al. No fitting to the alloy band structures was attempted. The onsite terms in the alloys were determined by the local charge neutrality approximation discussed in Sec. III B. The results are summarized in Table VII.

1. Fitting parameters for FCC nickel

The tight binding parameters for fcc Ni were chosen to reproduce the augmented plane wave (APW) band structure of paramagnetic Ni (Ref. 71) (and p. 19 of Papaconstantopoulos[72]). The error in ignoring the stabilizing effect of the ferromagnetic ground state is 0.05 eV, which is smaller than errors in the fit (0.1–0.2 eV). As the Ni p bands are largely unoccupied, a minimal s,d basis for Ni (i.e., no p orbital) was used to model the valence band structure. The fitting of the EHT parameters to the band structure requires a compromise between the widths of the pure (s-s and d-d) and mixed bands (s-d). The resulting fit has a d band that is 10% too narrow. The s-d hybridized band between Γ_{12} and X_4' is too broad near the X point. The largest errors are in states above and near the Fermi energy. As a consequence, the shape of the Fermi surface will not be accurately reproduced. However, the cohesive energy [Eqs. (7) and (8)] is determined by integrals over the entire valence band which have a smoothing effect. Provided the coarser features of the band (such as its width and asymmetry or skewness) are reproduced, the changes in local cohesive properties will also be reproduced. A more formal proof of this is given by the moments theorem.[73]

The minimal s,d basis cannot model the unoccupied states, except near the Fermi energy (within one to 2 eV). The Ni p states are not included in the EHT calculation as the Wolfsberg-Helmholtz approximation for H_{sp} greatly overestimated the s-p mixing in Ni. This leads to a large p

contribution near Γ_1 which should be almost purely *s* character (this problem can also be seen in the Ni DOS of Saillard and Hoffmann[74]). The combined interpolation scheme[75,76] where the *s* and *p* bands are modeled as a nearly free electron (NFE) gas and only the *d* states remain tightly bound (see Ref. 77) gives a better fit than the EHT method. A tight-binding–NFE Hamiltonian gives a remarkably good fit to APW calculations of Ni-Al.[78,79] This would be a very attractive method for future work if a real-space basis for the NFE gas could be found.

The EHT method should not be used for properties that rely quantitatively on the shape of the DOS directly (such as Fermi surface, transport properties, and EELS spectra away from threshold). It should, however, be acceptable to use the EHT method to simulate properties that rely on integrals over all occupied states, such as the cohesive energy, shifts in band centers and general trends in the shapes of the bands (such as the second, third, and fourth moments of the LDOS).

2. Fitting parameters for FCC aluminum

The tight-binding parameters for Al are taken from the *s*,*p* minimal basis fitted by Zheng and Hoffman[80] to the measured Al band structure.[81] The nonorthogonal *s* band has sufficient dispersion to reproduce the free-electron character of the band at low energies. However, the next three bands are not well reproduced. Although they have the correct width (important for reproducing the cohesive energy), in general, the energy gaps at the zone boundaries are overestimated. This is worst at the *X* point. The most obvious problem is that the dispersion of a second band between the X and W points has the wrong sign. For the same number of parameters (four), a nearly-free electron (NFE) model gives a better description of the band structure.[82,83].

Once again, the EHT band structure will not reproduce the Fermi surface or the optical spectrum of Al. However, as the bond energy involves an integral over all the occupied states, the states near the Fermi surface (which have the largest errors) make only a small contribution.

The EHT calculated DOS is shown in Fig. 5. While it reproduces the coarser features of the LMTO calculations at lower energies, the *p* states do not provide a good description of the higher energy states. However, the differences between the integrated densities of states are much smaller than differences between the densities of states themselves. The key point of Fig. 5 is that although the singular features are an important contribution to the single particle DOS, they do not have a significant effect on the *integrated* density of states.

[1] D. A. Muller, S. Subramanian, P. E. Batson, S. L. Sass, and J. Silcox, Phys. Rev. Lett. **75**, 4744 (1995).

[2] F. Ulrich Hillebrecht, J. C. Fuggle, P. A. Bennet, Z. Zolnierek, and C. Freiburg, Phys. Rev. B **27**, 2179 (1983).

[3] S. C. Lui, J. W. Davenport, E. W. Plummer, D. M. Zehner, and G. W. Fernando, Phys. Rev. B **42**, 1582 (1990).

[4] P. Fulde, *Electron Correlations in Molecules and Solids*, Springer Series in Solid-State Sciences. Vol. 100 (Springer-Verlag, Berlin, 1991).

[5] J. N. Murrell, S. F. Kettle, and J. M. Tedder, *The Chemical Bond*, 2nd ed. (Wiley, New York, 1985), p. 100.

[6] J. A. Rodriguez and D. W. Goodman, Science **257**, 897 (1992).

[7] M. Weinert and R. E. Watson, Phys. Rev. B **51**, 17 168 (1995).

[8] J. N. Andersen, D. Hennig, E. Lundgren, M. Methfessel, R. Nyholm, and M. Scheffler, Phys. Rev. B **50**, 17 525 (1994).

[9] P. Steiner and S. Hüfner, Acta Metall. **29**, 1885 (1981).

[10] A. Bzowski and T. K. Sham, Phys. Rev. B **48**, 7836 (1993).

[11] K. Karlsson, O. Gunnarsson, and O. Jepsen, J. Phys.: Condens. Matter **4**, 895 (1992).

[12] P. H. Citrin, G. K. Wertheim, and Y. Baer, Phys. Rev. Lett. **41**, 1425 (1978).

[13] P. H. Citrin and G. K. Wertheim, Phys. Rev. B **27**, 3176 (1983).

[14] D. E. Eastman, F. J. Himpsel, and J. F. van der Veen, J. Vac. Sci. Technol. **20**, 609 (1982).

[15] D. Hennig, M. V. Ganduglia-Pirovano, and M. Scheffler, Phys. Rev. B **53**, 10 344 (1996).

[16] D. G. Pettifor, Commun. Phys. **1**, 141 (1976).

[17] A. R. Mackintosh and O. K. Anderson, in *Electrons at the Fermi Surface*, edited by M. Springford (Cambridge University Press, London, 1980), Chap. 5.3.

[18] D. A. Muller, D. J. Singh, and J. Silcox, Phys. Rev. B **57**, 8181 (1998).

[19] C. Priester, G. Allan, and M. Lannoo, Phys. Rev. B **33**, 7386 (1986).

[20] A. P. Sutton, M. W. Finnis, D. G. Pettifor, and Y. Ohta, J. Phys. C **21**, 35 (1988).

[21] J. C. Cressoni and D. G. Pettifor, J. Phys.: Condens. Matter **3**, 495 (1991).

[22] R. Hoffmann, J. Chem. Phys. **39**, 1397 (1963).

[23] T. A. Koopmans, Physica (Amsterdam) **1**, 104 (1933).

[24] W. Kohn and L. J. Sham, Phys. Rev. **140**, A1133 (1965).

[25] V. Heine, in *Solid State Physics*, edited by H. Ehrenreich and F. Seitz (Academic Press, New York, 1980), Vol. 35, p. 1.

[26] A. P. Sutton and R. W. Balluffi, *Interfaces in Crystalline Materials* (Clarendon Press, Oxford, 1995).

[27] R. Wu, D. Wang, and A. J. Freeman, J. Magn. Magn. Mater. **132**, 103 (1994).

[28] P. Lerch, T. Jarlborg, V. Codazzi, G. Loupias, and A. M. Flank, Phys. Rev. B **45**, 11481 (1992).

[29] J. Hafner, in *The Structure of Binary Compounds*, edited by F. R. de Boer and D. G. Pettifor (North-Holland, Amsterdam, 1989), Vol. 2, p. 147.

[30] L. Hedin and A. Johansson, J. Phys. B **2**, 13366 (1969).

[31] O. K. Anderson, O. Jepsen, and D. Glotzel, in *Highlights of Condensed Matter Theory Course LXXXIX*, edited by F. Bassani, F. Fermi, and M. P. Tosi (North-Holland, Amsterdam, 1985).

[32] L. Hedin and S. Lundqvist, J. Phys. C **4**, 2064 (1971).

[33] O. K. Anderson, O. Jepsen, and M. Sob, in *Electronic Band Structure and its Applications*, edited by M. Yussouff, Lecture Notes in Physics Vol. 283 (Springer, Berlin, 1987).

[34] V. L. Moruzzi and P. M. Marcus, Phys. Rev. B **42**, 5539 (1990).

[35] T. Nautiyal and S. Auluck, Phys. Rev. B **45**, 13 930 (1992).

[36] P. Eckerlin and H. Kandler in *Landolt-Börnstein, New Series, Group III*, Vol. 6 Part X, edited by K. H. Hellewege (Springer-Verlag, New York, 1971).

[37] F. R. de Boer, C. J. Schinkel, J. Biesterbos, and S. Proost, J. Appl. Phys. **40**, 1049 (1969).
[38] D. Hackenbracht and J. Kubler, J. Phys. F **10**, 427 (1980).
[39] J. H. Xu, B. I. Min, A. J. Freeman, and T. Oguchi, Phys. Rev. B **41**, 5010 (1990).
[40] G. Lehmann and M. Taut, Phys. Status Solidi B **54**, 469 (1971).
[41] O. Jepsen, D. Glotzel, and A. R. Mackintosh, Phys. Rev. B **23**, 2684 (1981).
[42] M. Wolfsberg and L. Helmholtz, J. Chem. Phys. **20**, 837 (1952).
[43] R. Hoffmann, *Solids and Surfaces: A Chemist's View of Bonding in Extended Structures* (VCH Publishers, New York, 1988).
[44] D. G. Pettifor and R. Podloucky, J. Phys. C **19**, 285 (1986).
[45] D. G. Pettifor, Solid State Phys. **40**, 43 (1987).
[46] A. J. Skinner and D. G. Pettifor, J. Phys.: Condens. Matter **3**, 2029 (1991).
[47] L. C. Allen and J. D. Russell, J. Chem. Phys. **46**, 1029 (1967).
[48] M. O. Robbins and L. M. Falicov, Phys. Rev. B **29**, 1333 (1984).
[49] C. J. Ballhausen and H. B. Gray, *Molecular Orbital Theory, Frontiers in Chemistry Series* (W.A. Benjamin, New York, 1954).
[50] D. Nguyen-Manh, D. Mayou, A. Pasturel, and F. Cyrot-Lackman, J. Phys. F **15**, 1911 (1985).
[51] C. Colinet, P. Hicter, and A. Pasturel, Phys. Rev. B **45**, 1571 (1991).
[52] Additional documentation on *yaeht* and tight-binding parameters can be obtained from the Hoffman group, Chemistry Department, Baker Lab, Cornell University, Ithaca, NY 14853.
[53] A. E. Carlsson, Phys. Rev. B **44**, 6590 (1991).
[54] D. A. Muller and J. Silcox, Philos. Mag. A **71**, 1375 (1995).
[55] A. V. Crewe, J. Wall, and J. Langmore, Science **168**, 1338 (1970).
[56] N. D. Browning, M. M. Chisholm, and S. J. Pennycook, Nature (London) **366**, 143 (1993).
[57] P. E. Batson, Nature (London) **366**, 728 (1993).
[58] D. A. Muller, Y. Tzou, R. Raj, and J. Silcox, Nature (London) **366**, 725 (1993).
[59] P. E. Batson, Rev. Sci. Instrum. **57**, 43 (1986).
[60] L. Pauling, *The Nature of The Chemical Bond*, Springer Series in Solid-State Sciences (Cornell University Press, Ithaca, NY, 1960).
[61] K. Wong, Ph.D. thesis, Cornell University, Ithaca, NY, 1994.
[62] O. Bisi and C. Calandra, J. Phys. C **14**, 5479 (1981).
[63] C. Calandra, O. Bisi, and G. Ottaviani, Surf. Sci. Rep. **4**, 271 (1984).
[64] P. J. Grunthaner and F. J. Grunthaner, J. Vac. Sci. Technol. **20**, 680 (1982).
[65] A. Franciosi, J. H. Weaver, and F. A. Schmidt, Phys. Rev. B **26**, 546 (1982).
[66] R. E. Dietz, E. G. McRae, Y. Yafet, and C. W. Caldwell, Phys. Rev. Lett. **33**, 1372 (1974).
[67] W. A. Harrison, *Electronic Structure and the Properties of Solids* (Dover, New York, 1989).
[68] N. W. Ashcroft and N. D. Mermin, *Solid State Physics* (Saunder College Ed., Philadelphia, 1976).
[69] The off-diagonal matrix elements describes the tunneling (or ''hopping'') of the quasiparticle from one site to another. Wolfsberg and Helmholtz chose this form of H_{ij} so that the tunneling probability depends on the overlap of the wave functions, S_{ij}. The inclusion of the on-site terms is more difficult to justify, especially for the more localized *d* states (see Ref. 70).
[70] R. G. Woolley, Philos. Mag. B **69**, 745 (1994).
[71] L. F. Mattheiss, Phys. Rev. **134**, A970 (1964).
[72] D. A. Papaconstantopoulos, *Handbook of the Band Structure of Elemental Solids* (Plenum Press, New York, 1986).
[73] F. Cyrot-Lackmann, Adv. Phys. **16**, 393 (1967).
[74] J. Y. Saillard and R. Hoffmann, J. Am. Chem. Soc. **106**, 2006 (1984).
[75] L. Hodges and H. Ehrenreich, Phys. Rev. Lett. **16**, 20 (1965).
[76] F. M. Mueller, Phys. Rev. **153**, 659 (1967).
[77] D. G. Pettifor, J. Phys. C **5**, 97 (1972).
[78] R. Eibler and A. Neckel, J. Phys. F **10**, 2179 (1980).
[79] C. H. Muller, H. Wonn, W. Blau, P. Ziesche, and V. P. Krivitskii, Phys. Status Solidi B **95**, 215 (1979).
[80] C. Zheng and R. Hoffmann, Z. Naturforsch. B **41**, 292 (1986).
[81] H. J. Levinson, F. Greuter, and E. W. Plummer, Phys. Rev. B **27**, 727 (1983).
[82] N. W. Ashcroft, Philos. Mag. **8**, 2055 (1963).
[83] N. W. Ashcroft, Phys. Rev. B **19**, 4906 (1979).
[84] R. Hultgren and other, *Selected Values of the Thermodynamic Properties of Binary Alloys* (American Society for Metals, Metals Park, OH, 1973).